ANGEWANDTE
CHEMIE
A Journal of the
Gesellschaft
Deutscher Chemiker
INTERNATIONAL EDITION
2001
40/16
Pages 2935–3082

COVER PICTURE

The cover picture shows two new catalytic asymmetric reactions in front of an enantiomeric pair of lurs—one of the national symbols of Denmark. Chiral bisoxazoline copper complexes catalyze the reactions. The reaction on the left is the direct enantioselective Mannich reaction of carbonyl compounds with imines to give highly functionalized 4-oxo-glutamic esters, while the reaction on the right is the enantioselective nitro-Mannich reaction of nitro alkanes with imines to give optically active β-nitro-α-amino esters. Why the lur in relation to the present chemistry? Lurs exist as pairs of enantiomers and they probably belong to some of the first man-made pair of enantiomers, as they are from the Bronze Age (1000–500 BC). The lurs are the oldest musical instruments that can still be played, and are used as enantiomers. Side by side stood two lur-players, symmetric in every detail, the soft curves of the instruments swaying upwards and outwards at each side. The sonorous notes emphasized the solemn nature of the rituals. It is conceivable that the sound of the lur also accompanied the crackle of the funeral pyre when one of the tribe was cremated and laid to rest in the burial mound of his forefathers. The lurs are made of bronze (copper) and were discovered in lakes; less than 50 are known. The most famous pair of lurs was found in Brudevælte and is the pair shown on the cover. Further information about lurs can be obtained from kaj@chem.au.dk. The picture of the lurs and the accompanying music (click here to listen to the music: www.angewandte.com) are used with permission from The National Museum. For more details about the two new catalytic asymmetric reactions, see Jørgensen et al. on p. 2992 ff. and p. 2995 ff.

REVIEW

Spectroscopy at the working catalyst: Modern procedures of in situ spectroscopy are being increasingly applied to the preparation and selection of suitable reaction networks, the determination of the stoichiometry of individual intermediate steps of a network, and the identification and characterization of active centers, intermediates, the activation processes of the reactants, and the surface reactions. The picture exemplifies the changes in an IR spectrum during the course of a reaction.

Angew. Chem. **2001**, *113*, 3040 – 3059

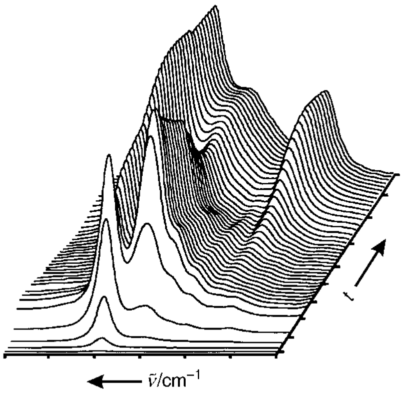

M. Hunger,* J. Weitkamp* .. 2954 – 2971

In situ IR, NMR, EPR, and UV/Vis Spectroscopy: Tools for New Insight into the Mechanisms of Heterogeneous Catalysis

Keywords: active centers · heterogeneous catalysis · in situ spectroscopy · reaction mechanisms · solid catalysts

HIGHLIGHTS

A window of opportunity: With the formation of a large orifice in the C_{60} core (**1**) and the successful insertion of He and H_2, two critical steps have been realized towards the development of an efficient synthetic approach for the preparation of endohedral fullerene complexes.

Angew. Chem. **2001**, *113*, 3061 – 3062

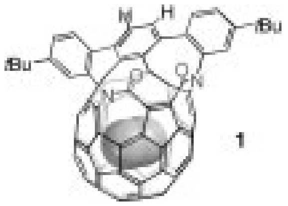

1

J.-F. Nierengarten* .... 2973 – 2974

Ring-Opened Fullerenes: An Unprecedented Class of Ligands for Supramolecular Chemistry

Keywords: fullerenes · host – guest systems · inclusion compounds · supramolecular chemistry

VIPs

The following communications are "Very Important Papers" in the opinion of two referees. They will be published shortly (those marked with a diamond will be published in the next issue). Short summaries of these articles can be found on the *Angewandte Chemie* homepage at the address http://www.angewandte.com

Synthesis of the C1 – C13 Fragment of Kendomycin: Atropisomerism around a C-Aryl Glycosidic Bond	H. J. Martin, M. Drescher, H. Kählig, S. Schneider, J. Mulzer*	◆
[$NdI_2(thf)_5$]: The First Crystallographically Authenticated Neodymium Complex	M. N. Bochkarev*, I. L. Fedushkin, S. Dechert, A. A. Fagin, H. Schumann*	◆
From Split-Pool Libraries to Spatially Addressable Microarrays and Its Application to Functional Proteomic Profiling	N. Winssinger, J. L. Harris, B. J. Backes, P. G. Schultz*	◆
High Turnover Numbers for Catalytic Selective Epoxidation of Alkenes with 1 atm Molecular Oxygen	Y. Nishiyama, Y. Nakagawa, N. Mizuno*	
Zero-Strain Intercalation Cathode for Rechargeable Li-Ion Cell	J. Cho, Y. J. Kim, T.-J. Kim, B. Park*	

1433-7851/01/4016-2938 $ 17.50+.50/0

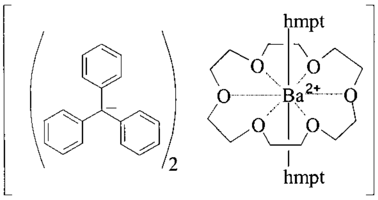

1

Even a century after the discovery of the Grignard reagents, similar compounds of the heavy alkaline earth metals are still lacking. Owing to the industrial need for such compounds (in particular as anionic polymerization catalysts), the last few years have been marked by a rapid, extensive development which has culminated in the first structurally characterized alkylbarium derivatives such as the crown ether complex of bis(triphenylmethyl)barium (**1**). hmpt = hexamethylphosphoric acid triamide.

Angew. Chem. **2001**, *113*, 3063 – 3065

M. Westerhausen* .... 2975 – 2977

100 Years after Grignard: Where Does the Organometallic Chemistry of the Heavy Alkaline Earth Metals Stand Today?

Keywords: alkaline earth metals · barium · calcium · carbanions · Grignard reactions

---

The visual pigment rhodopsin constitutes the interface between the physical event of light absorption and the biochemical process of visual transduction within the photoreceptor cells. The signal transduction is initiated by an 11-*cis* → all-*trans* photoisomerization of the retinal chromophore of rhodopsin which causes a series of thermally driven conformational changes of the chromophore and the protein moiety. A rhodopsin conformation is generated which allows interaction with a heterotrimeric G-protein (see picture). Two recent publications follow the chromophore motions after light absorption by cross-linking experiments and by solid-state NMR spectroscopy.

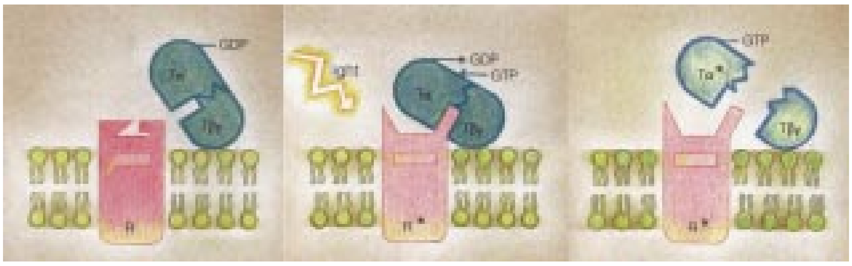

Angew. Chem. **2001**, *113*, 3065 – 3069

W. Gärtner* .... 2977 – 2981

The Light Shall Show the Way—Or: The Conformational Changes of the Retinal Chromophore in Rhodopsin upon Light Activation

Keywords: NMR spectroscopy · photochemistry · retinal · rhodopsin · signal transduction

COMMUNICATIONS

Simply decomposing InCp at room temperature in the presence of hexadecylamine leads to the formation of indium nanowires with a crystalline bct structure, a mean diameter of about 200 nm, and lengths in the micrometer range. The method can be extended to the preparation of In_3Sn nanowires of about 100 nm in diameter (a transmission electron micrograph is shown in the picture). $Cp = C_5H_5^-$.

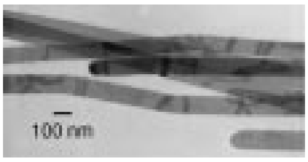

Angew. Chem. **2001**, *113*, 3072 – 3074

K. Soulantica, A. Maisonnat, F. Senocq, M.-C. Fromen, M.-J. Casanove, B. Chaudret* .... 2984 – 2986

Selective Synthesis of Novel In and In_3Sn Nanowires by an Organometallic Route at Room Temperature

Keywords: electron microscopy · indium · nanostructures · nanowires · tin

---

Enhanced global delocalization throughout the "stepped" π-electron systems of the [2.2]paracyclophane/dehydrobenzoannulene (PC/DBA) hybrids **1** and **2** is strongly suggested by a comparison of their electronic absorption spectra with those of model compounds with complete and interrupted classical aromatic delocalization. A distinct bathochromic shift (for **1**) and greater absorption intensity at higher wavelengths (for **1** and **2**) is observed versus the corresponding model hydrocarbons.

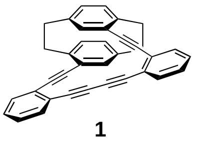

1

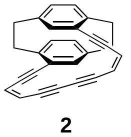

2

Angew. Chem. **2001**, *113*, 3074 – 3077

A. J. Boydston, L. Bondarenko, I. Dix, T. J. R. Weakley, H. Hopf,* M. M. Haley* .... 2986 – 2989

[2.2]Paracyclophane/Dehydrobenzoannulene Hybrids: Transannular Delocalization in Open-Circuited Conjugated Macrocycles

Keywords: alkynes · annulenes · aromaticity · cyclophanes · macrocycles

It is both an [18]trannulene and a [60]fullerene. It is aromatic and a hexa-substituted benzene. It is formed by the first proven example of an S_N2' reaction in a fullerene. It is intensely colored and stable. It is $C_{60}F_{15}[CBr(CO_2Et)_2]_3$, the first example of a new class of fullerene derivatives (see Schlegel diagram).

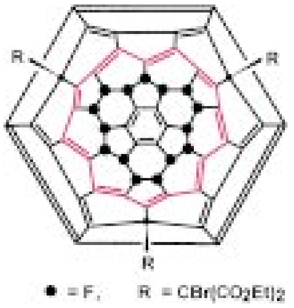

Angew. Chem. **2001**, *113*, 3077–3080

X.-W. Wei, A. D. Darwish,
O. V. Boltalina, P. B. Hitchcock,
J. M. Street, R. Taylor* 2989–2992

The Remarkable Stable Emerald Green $C_{60}F_{15}[CBr(CO_2Et)_2]_3$: The First [60]Fullerene That Is also the First [18]Trannulene

Keywords: annulenes • aromaticity • fluorine • fullerenes • nucleophilic substitution

---

The catalytic and asymmetric nitro-Mannich reaction of nitro compounds to α-imino esters catalyzed by chiral bisoxazoline–copper complexes [Eq. (1); Pg = protecting group] gave β-nitro-α-amino esters with excellent diastereo- and enantioselectivities. The reactions can be performed under ambient conditions.

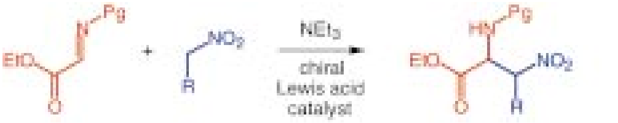

(1)

Angew. Chem. **2001**, *113*, 3080–3083

N. Nishiwaki, K. Rahbek Knudsen,
K. V. Gothelf,
K. A. Jørgensen* 2992–2995

Catalytic Enantioselective Addition of Nitro Compounds to Imines—A Simple Approach for the Synthesis of Optically Active β-Nitro-α-Amino Esters

Keywords: amino acids • asymmetric catalysis • imines • Lewis acids • nitro compounds

---

The development of a direct catalytic asymmetric Mannich reaction is shown and its potential demonstrated by the synthesis of optically active lactones via 4-hydroxyglutamic acid ester derivatives. The catalytic asymmetric Mannich reaction of carbonyl compounds with α-imino esters [Eq. (1); Ts = *p*-toluenesulfonyl] gives good yields and diastereoselectivities, as well as excellent enantioselectivities.

(1)

Angew. Chem. **2001**, *113*, 3083–3085

K. Juhl, N. Gathergood,
K. A. Jørgensen* 2995–2997

Catalytic Asymmetric Direct Mannich Reactions of Carbonyl Compounds with α-Imino Esters

Keywords: amino acids • asymmetric catalysis • imines • Lewis acids • Mannich reactions

---

A double shell of Platonic solids: A trajectory that connects the six-membered rings of I_h-C_{80} is followed by the two La atoms of $La_2@C_{80}$ according to maximum entropy/Rietveld analysis of the synchrotron powder-diffraction data. The result is a pentagonal-dodecahedral charge-density distribution for La_2 (brown in the picture) inside the icosahedral C_{80} cage (green).

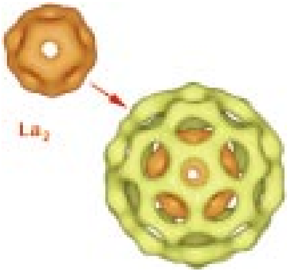

Angew. Chem. **2001**, *113*, 3086–3087

E. Nishibori, M. Takata,* M. Sakata,
A. Taninaka, H. Shinohara .. 2998–2999

Pentagonal-Dodecahedral La_2 Charge Density in [80-I_h]Fullerene: $La_2@C_{80}$

Keywords: fullerenes • lanthanum • structure elucidation • synchrotron radiation • X-ray diffraction

---

4-dimethylaminopyridine (DMAP) is the answer to the quest for an efficient transfer of metallic nanoparticles from organic to aqueous solutions. The picture shows the transfer of gold nanoparticles from toluene to water by the addition of DMAP (0.1M, pH 10.5). This method enables the generation of high concentrations of nanoparticles with better monodispersity than those commonly prepared in water.

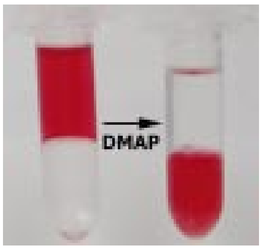

Angew. Chem. **2001**, *113*, 3089–3092

D. I. Gittins, F. Caruso* 3001–3004

Spontaneous Phase Transfer of Nanoparticulate Metals from Organic to Aqueous Media

Keywords: colloids • gold • nanostructures • phase-transfer catalysis • transition metals

1433-7851/01/4016-2940 $ 17.50+.50/0

A crucial role in the regulation of epithelial chloride secretion is played by the phosphoinositide PtdIns(3,4,5)P$_3$. Membrane-permeant derivatives of this and other naturally occurring phosphoinositides have been synthesized. These derivatives, which can be bioactivated, were used in investigations on nasal epithelia of patients suffering from cystic fibrosis (see general scheme).

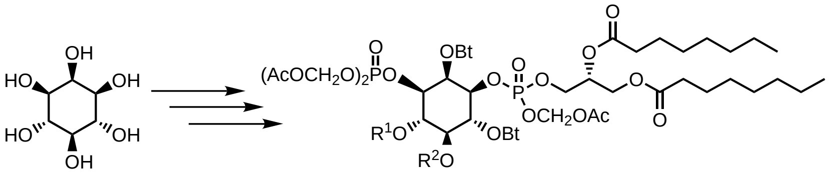

Angew. Chem. **2001**, *113*, 3093–3096

C. Dinkel, M. Moody,
A. Traynor-Kaplan,
C. Schultz* 3004–3008

Membrane-Permeant 3-OH-Phosphorylated Phosphoinositide Derivatives

Keywords: cyclitols · cystic fibrosis · phosphoinositides · secretion · signal transduction

---

Deep purple: By the transformation of readily available N,N-disubstituted 2-aminothiophenes and 2-aminothiazoles into heterocyclic analogues of Crystal Violet, such as, tris(2-dimethylamino-5-thienyl)methinium prechlorate (cation shown), the series of dyes derived from these heterocyclic structural units as the important chromophoric component is significantly extended and a gap in the class of heteroanalogous triphenylmethane dyes has been closed.

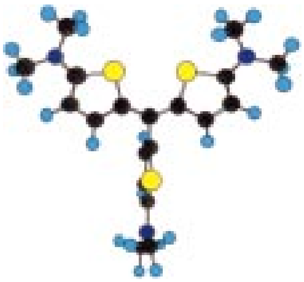

Angew. Chem. **2001**, *113*, 3097–3100

A. Noack, A. Schröder,
H. Hartmann* 3008–3011

Synthesis and Spectral Characterization of a New Class of Heterocyclic Analogues of Crystal Violet Dyes

Keywords: chromophores · Crystal Violet · dyes/pigments · sulfur heterocycles

---

The stabilizing effect of a dG:dC base-pair can also be imparted to a DNA duplex by a non-hydrogen-bonding, non-shape-complementary nucleoside analogue when inter-strand stacking interactions come into play. This is the case, for example, with dBP, which has a bipyridyl (BP) residue as a nucleobase surrogate (the picture shows a dBP:dBP pair).

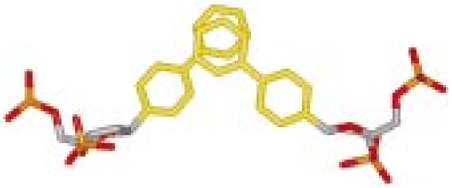

Angew. Chem. **2001**, *113*, 3101–3103

C. Brotschi, A. Häberli,
C. J. Leumann* 3012–3014

A Stable DNA Duplex Containing a Non-Hydrogen-Bonding and Non-Shape-Complementary Base Couple: Interstrand Stacking as the Stability Determining Factor

Keywords: DNA recognition · DNA structures · N ligands · nucleobases · oligonucleotides

---

Visible light can greatly enhance the oxidative degradation of organic compounds such as rhodamine B and salicylic acid, which are test compounds for organic pollutants. The degradations are significantly accelerated relative to reactions carried out in the dark. The mechanism involves the photoassisted generation of HO$^\bullet$ radicals, which react with the pollutants to form the degraded products.

Angew. Chem. **2001**, *113*, 3103–3105

X. Tao, W. Ma, T. Zhang,
J. Zhao* 3014–3016

Efficient Photooxidative Degradation of Organic Compounds in the Presence of Iron Tetrasulfophthalocyanine under Visible Light Irradiation

Keywords: EPR spectroscopy · iron · photochemistry · photodegradation · polluants

---

It was fortunate that the first extended branched polysilyl anion (Me$_3$SiMe$_2$Si)$_3$Si$^-$ could be crystallographically characterized in two forms—as the THF complex **1** and as the dimer **2**. Comparison with the analogous (Me$_3$Si)$_3$SiLi systems **3** and **4** shows that β-Me$_3$Si substitution and complexation by THF elongate the Si–Li distance by 0.09–0.14 Å and 0.04–0.07 Å, respectively.

$$\begin{tikzcd}
\underset{\mathbf{4}}{[(Me_3Si)_3Si\text{-}Li]_2} \arrow[r, dashed, "\Delta r = 0.12\text{-}0.14"] \arrow[d, dashed, "\Delta r \approx 0.07"] & \underset{\mathbf{2}}{[(Me_3SiMe_2Si)_3Si\text{-}Li]_2} \arrow[d, dashed, "\Delta r \approx 0.04"] \\
\underset{\mathbf{3}}{(Me_3Si)_3Si\text{-}Li\cdot 3THF} \arrow[r, dashed, "\Delta r = 0.09"] & \underset{\mathbf{1}}{(Me_3SiMe_2Si)_3Si\text{-}Li\cdot 3THF}
\end{tikzcd}$$

Angew. Chem. **2001**, *113*, 3106–3109

Y. Apeloig,* M. Yuzefovich,
M. Bendikov, D. Bravo-Zhivotovskii,*
D. Bläser, R. Boese 3016–3020

Branched Star-Type Polysilyllithium Compounds: The Effects of β-Silyl Substitution and of Complexation on Their Molecular Structure

Keywords: anions · density functional calculations · lithium · silicon

Semicrystalline microparticles of high molecular mass polyethylene can be prepared as aqueous dispersions (see picture) by catalytic emulsion polymerization of ethylene with a mini-emulsified catalyst precursor ($\overset{\frown}{\mathrm{D\,D}}$ = salicylaldimine, L = pyridine). Stable polymer latexes are formed.

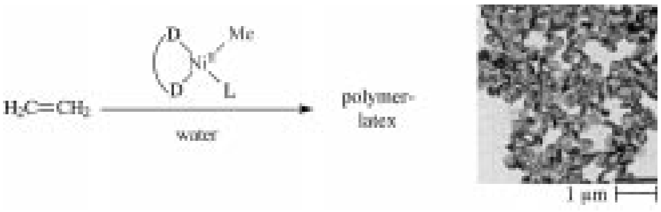

Angew. Chem. **2001**, *113*, 3112–3115

F. M. Bauers, S. Mecking* . 3020–3022

High Molecular Mass Polyethylene Aqueous Latexes by Catalytic Polymerization

Keywords: catalysis • colloids • dispersions • polyethylene • polymerization

---

By a sequence comprising asymmetric hydroboration, boron–zinc exchange, and transmetalation with copper, allylations, alkynylations, and allenylations of unsaturated ketals or acetals can be performed with good enantioselectivities (see scheme, (−)-IpcBH$_2$ = (−)-isopinocampheylborane, TMS = Me$_3$Si). The products correspond to a formal Michael addition with inversion of polarity.

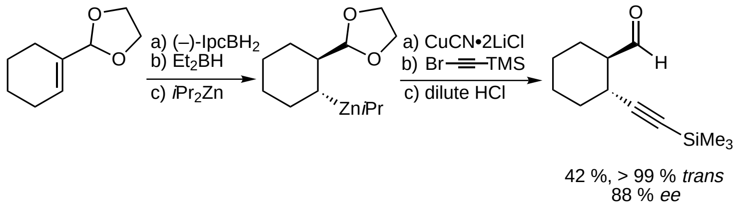

Angew. Chem. **2001**, *113*, 3109–3112

E. Hupe, P. Knochel* 3022–3025

Formal Enantioselective Michael Addition with Umpolung of Reactivity

Keywords: asymmetric synthesis • hydroboration • Michael addition • umpolung • zinc

---

The tautomeric four-membered-ring P–N heterocycles 1, **2**, and **3** can be interconverted; the formation of the cyclodiphosph(v)azene **1** is enthalpically and entropically favored. The crystal structures of the tautomers **1** and **3** have been determined and indications are given regarding the mechanism of the interconversion.

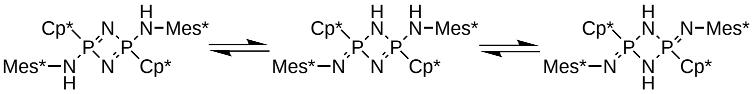

1 **2** **3**

Angew. Chem. **2001**, *113*, 3115–3117

J. Tirreé, D. Gudat, M. Nieger, E. Niecke* 3025–3028

Reversible Tautomeric Transformation between a Bis(amino)cyclodiphosph(v)azene and a Bis(imino)cyclodiphosph(v)azane

Keywords: NMR spectroscopy • phosphorus • phosphorus heterocycles • tautomerism

---

Rapid-scan FT-IR spectral imaging allows high-throughput screening of the activities of components of a catalyst library in a truly parallel fashion. The gas-phase reaction products from 16 supported catalysts can be investigated simultaneously with the reactor system described.

Angew. Chem. **2001**, *113*, 3117–3120

C. M. Snively, G. Oskarsdottir, J. Lauterbach* 3028–3030

Parallel Analysis of the Reaction Products from Combinatorial Catalyst Libraries

Keywords: catalysts • combinatorial chemistry • heterogeneous catalysis • high-throughput screening • vibrational spectroscopy

Cyano-mediated interaction of the alternating high-spin Mn^{II} centers and low-spin Ru^{III} centers in $\{Mn[Ru(acac)_2(CN)_2]_2\}_n$ (Hacac = acetylacetone) results in long-range ferromagnetic ordering below 3.6 K. This novel $Mn^{II}Ru^{III}$ coordination polymer, which has a diamond-like structure (see picture), was constructed from $[Ru(acac)_2(CN)_2]^-$ and Mn^{2+} ions.

Angew. Chem. **2001**, *113*, 3121 – 3123

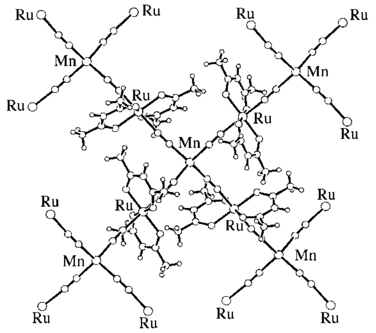

W.-F. Yeung, W.-L. Man, W.-T. Wong, T.-C. Lau,* S. Gao* .... 3031 – 3033

Ferromagnetic Ordering in a Diamond-Like Cyano-Bridged $Mn^{II}Ru^{III}$ Bimetallic Coordination Polymer

Keywords: coordination polymers · cyanides · magnetic properties · manganese · ruthenium

---

The unusually high kinetic stability of the silyl cation **1** is due to the presence of a three-center, two-electron Si-H-Si bond. NMR data (^1H, ^2H, ^{13}C, ^{29}Si) are consistent with the static, symmetrical structure shown, which was further corroborated by the results of density functional calculations.

Angew. Chem. **2001**, *113*, 3123 – 3126

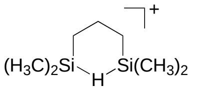

1

T. Müller* .... 3033 – 3036

A Silyl Cation with a Three-Center Si-H-Si Bond

Keywords: cations · density functional calculations · isotope effects · NMR spectroscopy · silicon

---

Oxo-like reactivity exists for a new series of osmium complexes such as $[Os^{IV}(bpy)(Cl)_3(NCN)]^-$ (bpy = 2,2′-bipyridine, see structure) containing the cyanoimido ligand. This ligand is formed directly at the metal center by the reaction of Os^{VI} – nitrido precursors with tetraethylammonium cyanide. In the cyanoimido complexes there is an extensive electron-transfer chemistry at the metal center and an extensive functional-group chemistry based on the ligand.

Angew. Chem. **2001**, *113*, 3127 – 3129

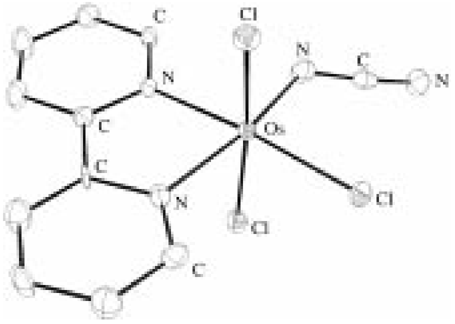

M. H. V. Huynh,* P. S. White, C. A. Carter, T. J. Meyer* ... 3037 – 3039

Formation and Reactivity of the Osmium(IV) – Cyanoimido Complex $[Os^{IV}(bpy)(Cl)_3(NCN)]^-$

Keywords: acylation · alkylation · cyanoimido ligands · osmium · protonation

---

First organic radicals, now metal complexes: A successful extension to metal complexes of a well-known organic radical approach to ferromagnetism is exemplified by the triplet ground-state molecule containing two Cu^{II} centers connected by a double *m*-phenylenediamide skeleton of the cyclophane type shown in the scheme.

Angew. Chem. **2001**, *113*, 3129 – 3132

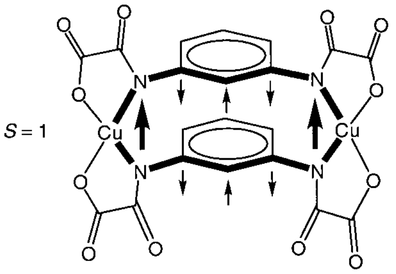

I. Fernández, R. Ruiz,* J. Faus, M. Julve, F. Lloret,* J. Cano, X. Ottenwaelder, Y. Journaux,* M. C. Muñoz . 3039 – 3042

Ferromagnetic Coupling through Spin Polarization in a Dinuclear Copper(II) Metallacyclophane

Keywords: amide ligands · copper · density functional calculations · magnetic properties · metallacycles

---

A triangle with a calixarene-like cone configuration: the trimetallamacrocycle $[\{Pd(en)(L)\}_3]^{6+}$ (**1**; L = *N,N′*-bis(4-dimethylaminophenyl)-1,4-benzoquinonediimine, en = ethylenediamine; see picture for a space-filling view). The coordination array of the redox-active π-conjugated bridging quinonediimine spacer of L and the palladium unit determines whether conjugated **1** or a conjugated polymeric complex is formed.

Angew. Chem. **2001**, *113*, 3132 – 3135

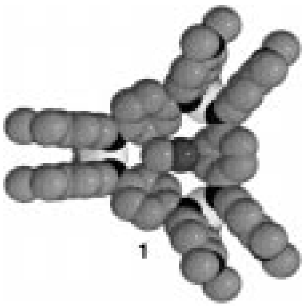

T. Moriuchi, M. Miyaishi, T. Hirao* .... 3042 – 3045

Conjugated Complexes Composed of Quinonediimine and Palladium: Controlled Formation of a Conjugated Trimetallic Macrocycle

Keywords: bridging ligands · coordination chemistry · macrocycles · palladium · stacking interactions

The covalent linkage of a hairpin polyamide, which binds in the minor groove, to camptothecin (see picture) provides an efficient system to direct topoisomerase I mediated DNA cleavage to specific sites. These conjugates are equally as potent at targeting the enzyme to a single site in a DNA fragment as camptothecin conjugates of ligands that bind in the major groove (triplex-forming oligonucleotides).

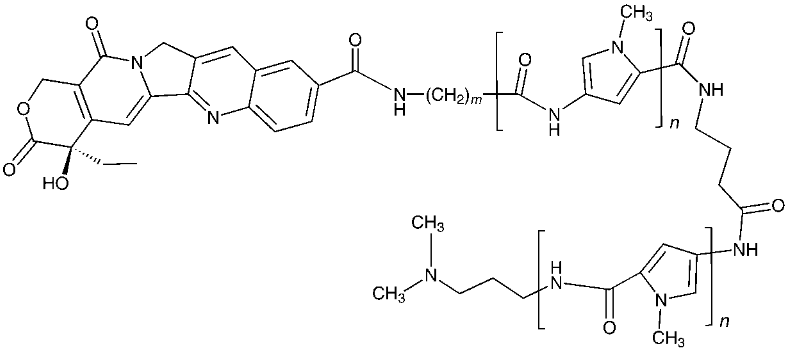

Angew. Chem. **2001**, *113*, 3135–3138

P. B. Arimondo, C. Bailly,
A. S. Boutorine, V. A. Ryabinin,
A. N. Syniakov, J.-S. Sun, T. Garestier,
C. Hélène* 3045–3048

Directing Topoisomerase I Mediated DNA Cleavage to Specific Sites by Camptothecin Tethered to Minor- and Major-Groove Ligands

Keywords: antitumor agents • DNA cleavage • DNA recognition • drug research • topoisomerase

---

Caged but not trapped! Caged reagents are molecules from which biological effectors are released by photolysis. Here, *p*-hydroxyphenacyl bromide is used to derivatize a model peptide containing a thiophosphotyrosine residue in order to mimic phosphorylation at tyrosine. Upon photolysis, a biologically active peptide is released. Peptides and proteins caged on thiophosphotyrosine will be useful in signal transduction research.

Angew. Chem. **2001**, *113*, 3139–3141

K. Zou, W. T. Miller, R. S. Givens,
H. Bayley* 3049–3051

Caged Thiophosphotyrosine Peptides

Keywords: bioorganic chemistry • peptides • photolysis • thiophosphate

---

The adhesion forces between individual molecules of Lewis^X trisaccharide antigen (Le^X) have been measured in water and in calcium solution by using atomic force microscopy (AFM, see graph). These results demonstrate the self-recognition capability of this antigen, and reinforce the hypothesis that carbohydrate–carbohydrate interaction could be considered as the first step in the cell-adhesion process in nature.

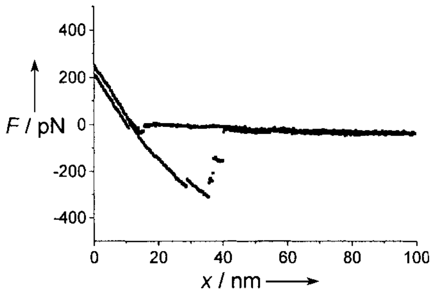

Angew. Chem. **2001**, *113*, 3142–3145

C. Tromas, J. Rojo, J. M. de la Fuente,
A. G. Barrientos, R. García,
S. Penadés* 3052–3055

Adhesion Forces between Lewis^X Determinant Antigens as Measured by Atomic Force Microscopy

Keywords: antigens • atomic force microscopy • carbohydrates • gold • noncovalent interactions

---

Pyrolysis of CH_3N_3 under the protection of NO generates a continuous methylnitrene CH_3N diradical beam that enables the ionization energies of different ionic states of the CH_3N diradical to be determined by HeI photoelectron spectroscopy (PES; see spectrum) and both ab initio and density functional theory (DFT) calculations. The ab initio and DFT results are in excellent agreement with the PES experiment and show that the CH_3N diradical has C_{3v} symmetry and the ground state of the CH_3N radical cation is the ^2E state.

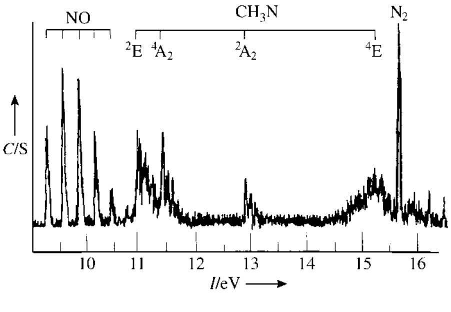

Angew. Chem. **2001**, *113*, 3145–3147

W. Jing, S. Zheng, Z. Xinjiang,
Y. Xiaojun, G. Maofa,
W. Dianxun* 3055–3057

The CH_3N Diradical: Experimental and Theoretical Determinations of the Ionization Energies

Keywords: ab initio calculations • density functional calculations • ionization potentials • nitrenes • photoelectron spectroscopy • radicals

Two cyclic Lewis acidic receptors, namely *B*-hexamethyl-9-mecuracarborand-3, $[9,12\text{-}(CH_3)_2\text{-}C_2B_{10}H_8Hg]_3$, each host a single water molecule. A benzene molecule is situated between the two complexed water molecules in a sandwich fashion that suggests there is O–H ⋯ π hydrogen bonding (see structure).

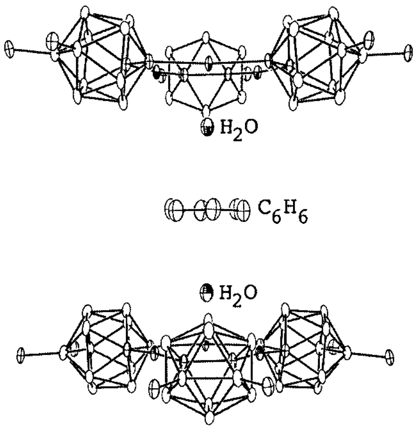

H. Lee, C. B. Knobler,
M. F. Hawthorne* 3058–3060

A Hydrogen-Bonded [(Mercuracarborand–Water)$_2$–Benzene] π-Sandwich Complex

Keywords: carboranes · host–guest systems · hydrogen bonds · pi interactions · sandwich complexes

Angew. Chem. **2001**, *113*, 3148–3150

Old problems, new ideas! The biomimetic phenol coupling of norbelladine derivatives such as **1** (Bn = benzyl) to form galanthamine (**2**), a drug used in the treatment of Alzheimer's disease, has been greatly improved by the use of the hypervalent-iodine oxidation reagent phenyliodine(III) bis(trifluoroacetate) (PIFA).

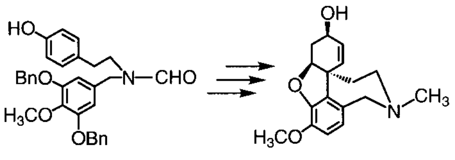

1 2

M. Node,* S. Kodama, Y. Hamashima,
T. Baba, N. Hamamichi,
K. Nishide 3060–3062

An Efficient Synthesis of (±)-Narwedine and (±)-Galanthamine by an Improved Phenolic Oxidative Coupling

Keywords: biomimetic synthesis · drug research · enzyme inhibitors · iodine reagents · oxidation

Angew. Chem. **2001**, *113*, 3150–3152

Instant radiopharmaceuticals—just add $[^{99m}TcO_4]^-$ in water! Half-sandwich complexes of the type $[(RCOCp)^{99m}Tc(CO)_3]$ (e.g. **1**) were synthesized in a single step in water from $[^{99m}TcO_4]^-$. The acidification of the Cp ring by a carbonyl substituent and the use of $K_2[H_3BCO_2]$ as a reducing agent and in situ source of CO are instrumental in the synthesis.

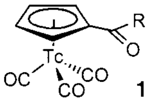

1

J. Wald, R. Alberto,* K. Ortner,
L. Candreia 3062–3066

Aqueous One-Pot Synthesis of Derivatized Cyclopentadienyl–Tricarbonyl Complexes of ^{99m}Tc with an In Situ CO Source: Application to a Serotonergic Receptor Ligand

Keywords: carbonylation · cyclopentadienyl ligands · radiopharmaceuticals · rhenium · technetium

Angew. Chem. **2001**, *113*, 3152–3156

Displacement of the loosely encapsulated fluorescent indicator coumarine 343 (F) from a dicopper(II) cryptate enables the selective fluorimetric detection of the HCO_3^- ion (A) in water (see scheme, ● = Cu^{2+}). The fluorophore is quenched when encapsulated, but displays its full emission when released to the solution.

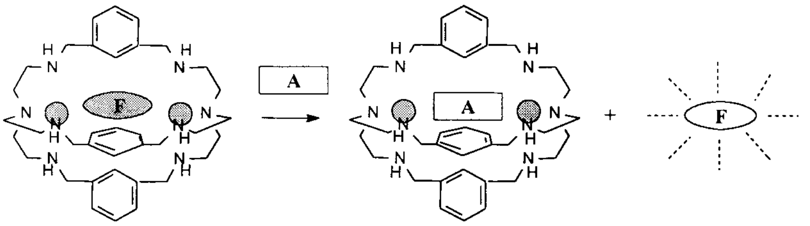

L. Fabbrizzi,* A. Leone,
A. Taglietti 3066–3069

A Chemosensing Ensemble for Selective Carbonate Detection in Water Based on Metal–Ligand Interactions

Keywords: anions · cryptates · fluorescence spectroscopy · molecular recognition · sensors

Angew. Chem. **2001**, *113*, 3156–3159

1433-7851/01/4016-2945 $ 17.50+.50/0

Lattices of single polystyrene particles were constructed by using a combinatorial approach to analyze particle pattern recognition properties. Dip-pen nanolithography was used to generate chemical templates of 16-thiohexadecanoic acid on a gold surface to study the two-dimensional assembly of amine- and amidine-modified particles (see picture).

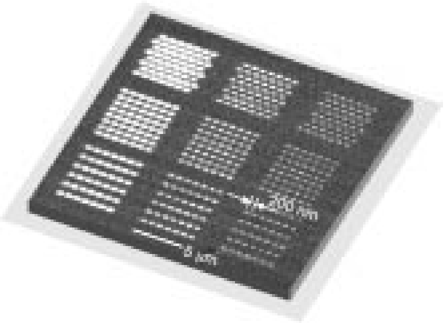

Angew. Chem. **2001**, *113*, 3159–3161

Nanoscale construction work with DNA: Dip-pen nanolithography (DPN) is used to generate nanostructures which can be subsequently functionalized with oligonucleotides **a′** and **b′** and used to assemble, in an orthogonal manner, gold nanoparticles (**a**, **b** in scheme) functionalized with sequences complementary to the DPN-generated structures.

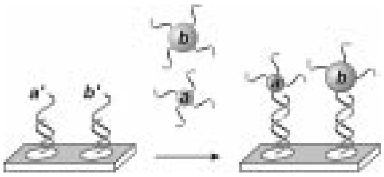

Angew. Chem. **2001**, *113*, 3161–3163

Supporting information on the WWW (see article for access details).

* Author to whom correspondence should be addressed

BOOKS

WEB SITES

Don't forget all the Tables of Contents from 1998 onwards may be still found on the WWW under: http://www.angewandte.com

CORRIGENDA

The assignment of the ^{15}N NMR signals of N_5^+ in the Communication by **K. O. Christe et al.** in Issue 13/14, 1999, pp. 2004–2010 were inadvertently reversed. The signal at $\delta = -237.3$ (calculated: -235) corresponds to the central N atom N3, and that at $\delta = -100.4$ (calculated: -95) to N1 (see for example Table 1 in this contribution).

The ^{13}C NMR data given in the Communication by **R. Langer et al**. in Issue 4, 2001, pp. 726–728 for dinitro[2.2]paracyclophane **2b** were for a mixture of isomers. Data for the pseudo-*para* isomer as well as revised data for the nitro[2.2]paracyclophane **2a** and the amino[2.2]paracycophane **3a** are given here.

2a: $\delta = 34.36, 34.69, 34.91, 35.93, 129.45, 129.86, 132.31, 133.07, 133.12, 136.37, 137.27, 137.73, 139.26, 139.68, 142.02, 149.17$.
2b: $\delta = 34.17, 34.60, 129.13, 133.87, 136.46, 137.36, 142.00, 149.71$.
3a: $\delta = 32.23, 33.03, 34.95, 35.37, 122.36, 122.99, 124.60, 126.82, 131.48, 132.43, 133.23, 135.44, 138.91, 138.97, 141.06, 144.72$.

In the Comunication by **M. F. Hawthorne et al.** in Issue 9, 2001, pp. 1661–1664 there was an error in the equation at the top of the frontispiece: it should read R^2_2O not $(R^2CO)_2O$, and the text at the bottom the page should read "Globular molecules with an icosahedral core—12(12)-closomers—are obtained by total esterification and etherification of $[B_{12}(OH)_{12}]^{2-}$. For details as well as for the transformation of an anionic closomer ether into the neutral *hypercloso* analogue see the following two communications". An error in Scheme 1 was also inadvertently introduced; the correct scheme is given here.

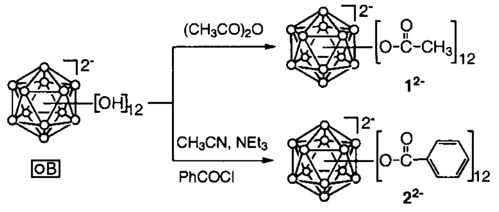

In the Communication by **G. de Petris et al**. in Issue 10, 2001, pp. 1938–1941 complexes **1** and **2** in Equations (3) and (4) were erroneously written. The correct Equations are given here.

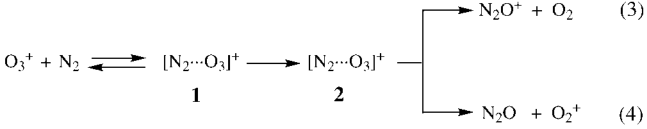

$$O_3^+ + N_2 \rightleftharpoons \underset{\mathbf{1}}{[N_2\cdots O_3]^+} \longrightarrow \underset{\mathbf{2}}{[N_2\cdots O_3]^+} \longrightarrow \begin{cases} N_2O^+ + O_2 & (3) \\ N_2O + O_2^+ & (4) \end{cases}$$

In the minireview by **P. Braunstein** and **N. M. Boag** in Issue 13, 2001, pp. 2427–2433 the isolobal signs were inadvertently missing from the second sentence of the abstract, the second sentence should read:
The C, Si, and P donor atoms of these ligands are sp^3-hybridized and the ligands are related to each other by the isolobal analogy: $(CR_3)^- \underset{\circ}{\longrightarrow} (SiR_3)^- \underset{\circ}{\longrightarrow} PR_3$.
We would like to apologize for this error.

In the communication by **Y. Gu et al.** in Issue 12, 2001, pp. 2320–2322 the protein surface coverages listed in Table 1 were incorrect. Since that publication, the authors identified and corrected a systematic error in the method used to determine surface coverages. The corrected Table is given here. The corrected data show that a spacer arm of three ethylene glycol units (in Gal-**3**) is sufficient for rgp120 recognition of a galatosyl receptor presented at the surface of a planar DOPC membrane. Longer spacer arm lengths (in Gal-**4** and -**5**) result in less efficient recognition. The authors apologize for this error.

Table 1. Summary of rgp120 binding behavior at planar DOPC membranes, either pure or doped with 5 % (mol mol^{-1}) of Gal-**3**, -**4**, or -**5** in the outer leaflet.[a]

	DOPC	Gal-**3**	Gal-**4**	Gal-**5**
K_a ($\times 10^6$)	–	5.4 ± 1.8	3.8 ± 0.57	2.5 ± 0.57
cooperativity coefficient (ω)	–	1.44 ± 0.20	1.50 ± 0.28	1.59 ± 0.11
surface coverage [mol cm^{-2} $\times 10^{-13}$][b]	1.6 ± 0.23	3.6 ± 0.57	2.2 ± 0.19	2.2 ± 0.13

[a] All values listed are the mean and standard deviation of two experimental trials. [b] Surface coverages were determined at a dissolved rgp120 concentration of 208 nM, using a modification of the method described by Haldy et al.[26]